KINETICS OF DIFFUSION-CONTROLLED AND BALLISTICALLY-CONTROLLED REACTIONS

S. REDNER
Center for Polymer Studies and Department of Physics, Boston University
Boston, MA 02215, USA

ABSTRACT

The kinetics of diffusion-controlled two-species annihilation, $A+B\to 0$ and single-species ballistically-controlled annihilation, $A+A\to 0$ are investigated. For two-species annihilation, we describe the basic mechanism that leads to the formation of a coarsening mosaic of A- and B-domains. The implications of this picture on the distribution of reactants is discussed. For ballistic annihilation, dimensional analysis shows that the concentration and rms velocity decay as $c\sim t^{-\alpha}$ and $v\sim t^{-\beta}$, respectively, with $\alpha+\beta=1$ in any spatial dimension. Analysis of the Boltzmann equation for the evolution of the velocity distribution yields accurate predictions for the kinetics. New phenomena associated with discrete initial velocity distributions and with mixed ballistic and diffusive reactant motion are also discussed.

1. Introduction

In this article, we describe some intriguing kinetic and geometric properties of diffusion-controlled two-species annihilation, $A + B \to 0$, in which an encounter between two distinct species A and B leads to the formation of an inert product, and single-species ballistically-controlled annihilation, $A+A \to 0$, in which particles move ballistically until reaction. In the former case, when the two species are spatially uniform and present in equal concentrations initially, there is a spontaneous symmetry breaking where large-scale single species heterogeneities form.[1-4] One way to describe the mechanism underlying this domain formation is that nearby AB pairs will quickly annihilate, giving rise to an effective "repulsion" which favors keeping AB pairs relatively well separated. In low spatial dimension, this effective repulsion dominates over the mixing due to diffusion. The resulting spatial organization invalidates the mean-field approximation and its corresponding predictions. One of our goals is to outline the consequences of this spatial organization.

The contrasting situation where reactants move ballistically has received much less attention and the scope of current knowledge is correspondingly sparser.[5-8] Here, we present several new results for the kinetics of single-species annihilation, $A + A \to 0$ when the rate limiting step of the process is the ballistic transport of reactants. This ballistically-controlled situation appears simpler than its diffusion-controlled counterpart, since the only stochasticity in the process is the initial velocity distribution of the reactants. However, rich and unanticipated phenomena occur which depend on the form of the initial velocity distribution. We will also describe some of the particularly intriguing phenomena that arise in systems with discrete initial velocity distributions. Finally, we give a scaling argument to determine the

kinetics of the $A + A \to 0$ reaction under the combined influence of diffusion and ballistic motion. Interestingly, the decay in this composite situation is faster than that of either pure ballistic motion or pure diffusive motion.

2. Diffusion-Controlled Two-Species Annihilation

2.1. Decay of the Density

Consider two diffusing species A and B which are originally distributed at random with respective concentrations $c_A(0)$ and $c_B(0)$. When two opposite species particles approach within the reaction radius, they react irreversibly to form an inert species. When the initial concentrations of the two species are equal, $c_A(0) = c_B(0) \equiv c(0)$, then $c(t)$ decays as a power law in time and there is a large-scale spatial organization of reactants in low spatial dimensions.

To estimate the decay of the density within a mean-field approximation, note that in a time interval of order $1/c$, each particle will come in contact with another particle, on average. Consequently, in a time interval $\Delta t \propto 1/kc$, where k is the reaction rate, the concentration will decrease by an amount of order c, that is, $\Delta c \propto -c$. This gives the mean-field rate equation

$$\dot{c} \cong \frac{\Delta c}{\Delta t} \propto -kc^2, \tag{1}$$

with solution $c(t) = c(0)/(1 + kc(0)t) \sim (kt)^{-1}$. Thus the exponent of the decay is -1, and the time scale is set by k. This exponent value turns out to be correct only for spatial dimension $d \geq 4$, corresponding to the regime of validity of the mean-field prediction. On the other hand, for spatial dimension $d < 2$ the time interval for reactions to occur is now $\Delta t \propto \ell^2/D$, where $\ell \propto c^{-1/d}$ is the typical interparticle spacing and D is the diffusion coefficient. Notice that the reaction rate does not enter into this time scale because random walk trajectories are compact. Therefore if two reactants collide once, they will collide an infinite number of times and the reaction rate rescales to a large value. Consequently, for $d < 2$ the rate equation now becomes,

$$\dot{c} \cong \frac{\Delta c}{\Delta t} \propto -Dc^{1+2/d}, \tag{2}$$

with solution $c(t) \sim (Dt)^{-d/2}$.

For $d \leq 4$, both of the above predictions for $c(t)$ are incorrect because domains which contain only one of the two species form, thus invalidating the homogeneity assumption of the mean-field approximation. Explicit account of the local density fluctuations are needed to understand the long-time behavior of $c(t)$.[5–8] This can be accomplished by noting that the difference in the number of A's and B's in a finite volume Ω of linear dimension L remains nearly constant during the time for a particle to traverse the volume by diffusion, $t_L \sim L^2/D$. At $t = 0$, this difference is of the order to the square root of the initial particle number,

$$N_A - N_B \approx \pm\sqrt{c(0)}\; L^{d/2}. \tag{3}$$

If we assume that A's are initially the local majority in Ω, then for $d \leq 4$, essentially no B's will remain after a time t_L has elapsed. Thus $N_A(t_L)$ is approximately equal to $\sqrt{c(0)}\, L^{d/2}$. Elimination of L in favor of t gives,

$$c(t) \approx N(t)/L^d \sim \sqrt{c(0)}\ (Dt)^{-d/4}, \qquad (d \leq 4). \tag{4}$$

Thus a homogeneous system is predicted to evolve into a mosaic of continuously growing domains whose individual identities are determined by the species in the local majority in the initial state. At time t, these domains will be of typical linear dimension $\sqrt{Dt}$, within which a single species of density $\sqrt{c(0)}\ (Dt)^{-d/4}$ remains.

The above line of reasoning is invalid for $d > 4$, however. To appreciate what occurs in this case, consider the stability of a reaction-generated domain mosaic for $d > 4$. For this purpose, we estimate the probability that an A particle is unsuccessful in crossing a typical B domain of linear dimension L and local concentration of order $L^{-d/2}$. For $d > 4$, the particle needs L^2 time steps to cross the domain and will visit L^2 distinct sites during the traversal. At each site, the A will react with a probability that is of the order of the B concentration, $L^{-d/2}$. Therefore the probability that an A particle is unsuccessful in traversing a B domain is of the order of $L^{(4-d)/2}$. Since this vanishes as $L \to \infty$ if $d > 4$, the domain mosaic is unstable to diffusion for $d > 4$.

Thus for $d < 4$, the kinetics of the $A + B \to 0$ reaction is determined by the competition between A- and B-domains. This process depends fundamentally on geometric features of these domains, such as the interparticle distances between closest-neighbor like and unlike species and the domain size distribution. Some unexpected properties emerge from these quantities as we now discuss.

2.2. The "Gap" Distance

One surprising feature of the spatial distribution of reactants is that for $d < 3$ the typical distances between AA and AB closest-neighbor pairs, ℓ_{AA} and ℓ_{AB}, respectively, grow with different powers of time.[9] The latter characterizes the width of the "gap" that separates adjacent domains (Fig. 1). The different scaling of the two

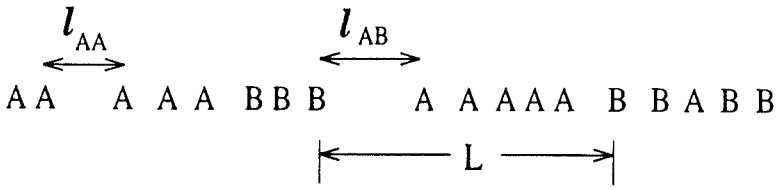

Figure 1. Definition of fundamental interparticle distances in one dimension: the typical distance between closest-neighbor same species particles, ℓ_{AA}, the distance between closest-neighbor unlike species, ℓ_{AB}, (the gap between domains), and the typical domain length, L.

lengths indicates that there is a non-trivial modulation in the reactant density over the extent of a domain. To determine the time evolution of ℓ_{AB} in one dimension,

consider the behavior of c_{AB}, the concentration of closest-neighbor AB pairs. In a time increment $\Delta t \sim \ell_{AB}^2/D$, there is sufficient time for essentially all such AB pairs to react, since one-dimensional random walks are compact. Consequently, the number of reactions per unit length is of the order of c_{AB}. Thus the rate of change of the concentration is

$$\frac{\Delta c}{\Delta t} \approx -k \frac{c_{AB}}{\ell_{AB}^2/D}. \tag{5}$$

This relation holds only for spatial dimension $d < 2$, since the compactness of random walks is an essential ingredient in the argument. Since we independently know the left-hand side of Eq. (5) from $c(t)$ itself, the behavior of c_{AB} determines the time dependence of ℓ_{AB}. In one dimension, c_{AB} scales as $(Dt)^{-1/2}$, since there is one AB pair per domain of typical size $(Dt)^{1/2}$. Therefore

$$\ell_{AB} \sim c(0)^{-1/4} \, (Dt)^{3/8}. \tag{6}$$

Thus at least three lengths are needed to characterize the spatial distribution of reactants: the average domain size, which scales as $(Dt)^{1/2}$; the typical interparticle spacing, which scales as $c(t)^{-1} \propto t^{1/4}$; and the interdomain gap ℓ_{AB}. The stronger time dependence of ℓ_{AB} compared to that of the typical interparticle spacing is a manifestation of an effective "repulsion" between opposite species particles. Nearby opposite species pairs annihilate preferentially, leaving behind a population where opposite species are separated by a distance which is larger than the typical interparticle separation.

To generalize to spatial dimension $1 \leq d \leq 2$, note that the time dependence of ℓ_{AB} should still follow by applying Eq. (5), since it holds whenever random walks are compact. To estimate c_{AB}, we assume a smooth domain perimeter of length $t^{(d-1)/2}$ and that particles in the perimeter zone are separated by a distance of the order of ℓ_{AB}, irrespective of identity. This straightforwardly leads to the following generalization of Eq. (6),

$$\ell_{AB} \propto t^{\frac{(d+2)}{4(d+1)}}, \qquad c_{AB}(t) \propto t^{-\frac{d(d+3)}{4(d+1)}}, \tag{7}$$

which yields $\ell_{AB} \sim t^{1/3}$ and $c_{AB}(t) \sim t^{-5/6}$ in $d = 2$.

In three and higher dimensions, the transience of random walks implies that two neighboring opposite species particles which are confined to a region of linear dimension ℓ_{AB} will react within a time of the order of ℓ_{AB}^d (rather than ℓ_{AB}^2). Consequently, Eq. (5) must be modified to

$$\frac{\Delta c}{\Delta t} \approx -k \frac{c_{AB}}{\ell_{AB}^d}. \tag{8}$$

This relation, together with the assumption of a smooth interfacial region between domains, gives, in d dimensions:

$$c_{AB} \approx t^{-\frac{d^2+5d-4}{4(2d-1)}}, \qquad \ell_{AB} \approx t^{\frac{d+2}{4(2d-1)}}, \tag{9}$$

which coincides with Eq. (7) at $d = 2$. For $d = 3$, Eq. (9) yields

$$c_{AB} \approx t^{-1}, \qquad \ell_{AB} \approx t^{1/4}. \tag{10}$$

These exponents represent limiting values, as there is no mechanism whereby $\langle \ell_{AB} \rangle$ could become less than $\langle \ell_{AA} \rangle$. Thus the non-trivial scaling of interparticle distances disappears in three dimensions and above and there is no appreciable depletion in the average density in the interfacial region between domains. The existence of a critical dimension of 3 for the behavior of the interparticle distances is striking, as the upper critical dimension equals 4 for the behavior of $c(t)$.

2.3. The Domain Profile and Interparticle Distance Distribution

A revealing physical picture for the spatial distribution of the reactants can be obtained from the average density profile of the domains. It is natural to define a "microcanonical" density profile, $P^{(M)}(x)$, as the probability of finding a particle at a scaled distance x from the domain midpoint, when each domain is scaled to a *fixed* size. The resulting profile is a flattened sinusoid. To understand this result, note that the long-time probability distribution for pure diffusion in a fixed size absorbing domain is a pure sinusoid. For an absorbing domain $[-L(t), L(t)]$ with $L(t) \propto t^{1/2}$ the adiabatic approximation marginally applies,[10] from which the density profile is $\cos(\pi x/L(t))$ (as in the case of a static absorbing domain). A more faithful model to account for the stochastic motion of the domain walls. Thus consider the extreme particle in each of the two enclosing domains to be wall particles W, with the A's and W's reacting via $W + W \to I$ and $W + A \to W$ to describe two-species annihilation. This mapping to an exactly-soluble three-particle system[11] of a single A between two W's neglects the possibility that a W particle can disappear in an encounter with another W before reacting with the A. Proceeding nevertheless, we postulate that the motion of the W's is diffusive, from which the determination of the density profile of the A's reduces to obtaining the probability distribution of a random walker between the two absorbing wall particles. The exact solution to this three-particle problem again predicts the profile $\cos(\pi x/L(t))$, independent of the diffusion coefficients of the A's and W's.

The inhomogeneous domain profile also governs the distribution of interparticle distances. Particles are separated by the typical interparticle separation which grows as $t^{1/4}$ within the core of the domain, but systematically become more sparse as the domain edge is approached, with the density decaying *linearly* to zero. The core and the interfacial region each comprise a finite fraction of the domain size. This large-scale modulation in the interparticle spacings leads to an interparticle distance distribution which is controlled both by the gap length ℓ_{AB} and the typical spacing between same species particles ℓ_{AA}.

Very roughly, these essential features of the scaled domain profile can be accounted for by the following trapezoidal form (Fig. 2),

$$\rho(z) \equiv c(x,t)\, t^{1/4} = \begin{cases} \rho_0, & |z| \le z^*; \\ \rho_0(1 - |z|), & z^* < |z| < 1 - \epsilon. \end{cases} \tag{11}$$

Here ρ_0 and z^* are constants, with z^* less than, but of order unity, and z is the scaled spatial co-ordinate, defined by $z = x/L(t)$, with $x \in [-L(t), L(t)]$. The upper limit for $|z|$ on the second line of Eq. (11) reflects the fact that there are no particles within a scaled distance of $\epsilon \equiv \ell_{AB}/L(t) \sim t^{-1/8}$ from the domain edge.

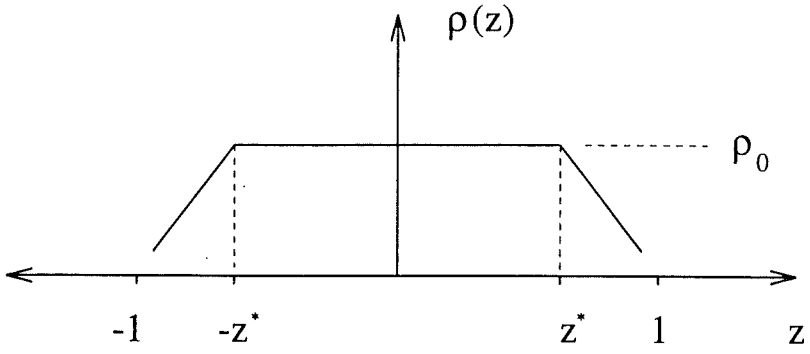

Figure 2. Idealized trapezoidal form which accounts for the scaling properties of the actual microcanonical density profile of a single domain. In the core of the domain, the density is relatively constant, while the density vanishes linearly as a function of the distance to the domain edge.

From this idealized trapezoidal profile, we can determine both the functional form of the probability distribution of finding adjacent AA pairs with separation x, $P_{AA}(x,t)$, and the time dependence of the corresponding reduced moments, $M_n \equiv \langle \ell_{AA}^n \rangle^{1/n}$, defined by

$$\langle \ell_{AA}^n \rangle = \int_0^\infty x^n \, P_{AA}(x,t) \, dx. \tag{12}$$

From this trapezoidal distribution, the n^{th} moment of the nearest-neighbor distance between same-species particles is obtained by the following average of the local nearest-neighbor distance over the extent of the domain

$$M_n \approx t^{1/4} \times \left(2 \int_0^{z*} \frac{dz}{\rho_0^n} + 2 \int_{z*}^{1-\epsilon} \frac{dz}{\rho_0^n (1-z)^n} \right)^{1/n}. \tag{13}$$

A crucial feature of the averaging is that the local nearest-neighbor distance is simply $\rho(z)^{-1}$, with $\rho(z) = \rho_0$ in the domain core ($|z| \leq z^*$), but with $\rho(z) = \rho_0(1 - |z|)$ near the domain boundary. As a result, the dominant contribution to M_n originates from different terms in Eq. (13) as n is varied. For $n < 1$, the integral is dominated by the first (constant) term in the parentheses, while for $n > 1$, the second term dominates the entire expression. (For $n = 1$, the second term gives rise to a logarithmic singularity at the upper limit.) We thereby obtain from Eq. (13),

$$M_n \sim \begin{cases} t^{1/4}, & n < 1; \\ t^{1/4} \ln t, & n = 1; \\ t^{(3n-1)/8n}, & n > 1. \end{cases} \tag{14}$$

Thus there is a logarithmic factor in the ratio between the average and typical distance between nearest-neighbor particles of the same species, and a power-law diverging factor for the higher moments. As $n \to \infty$, the reduced moment is dominated by the contribution from the sparsely populated region near the periphery of the domain where nearest-neighbor particles are separated by a distance that grows as $t^{3/8}$.

Rather unusual behavior occurs when one species (B) is immobile.[9] Regions of initially closely-spaced B's give rise to an $x^{-3/2}$ tail in the probability of finding a BB closest-neighbor distance equal to x for $x < t^{1/2}$. For such a distribution, the time dependence for the reduced moments of interparticle distances between the immobile species is

$$M_n(t) \sim \begin{cases} \text{const.}, & n < 1/2; \\ \ln t, & n = 1/2; \\ t^{(2n-1)/4n}, & n > 1/2. \end{cases} \tag{15}$$

Due to the relatively large number of small BB distances, the reduced moments of order less than $1/2$ have a finite limiting value as $t \to \infty$, while higher-order moments grow indefinitely and are dominated by very large BB distances of the order of $t^{1/2}$. These results are indicative of a fractal spatial distribution for the immobile species.

To generalize the interparticle distance moments to higher dimensions for equally mobile species, we treat the density profile as the probability distribution of a particle diffusing within an absorbing sphere whose radius expands as $\sqrt{t}$. The adiabatic approximation still applies in this case, so that the density should decay linearly to zero in the radial coordinate near the extremity of the domain. By following a calculation in the same spirit as in one dimension, we find the reduced moments $M_n(t)$ to be,

$$M_n(t) \sim \begin{cases} t^{1/4}, & n < 2; \\ t^{1/4}(\ln t)^{1/2}, & n = 2; \\ t^{(2n-1)/6n}, & n > 2. \end{cases} \tag{16}$$

These predictions for $d > 1$ have yet to be adequately tested, however. This stems, in part, to the algorithmic difficulty in defining a domain in higher dimensions. It is natural is to define a microcanonical density profile by superposing the profiles from one-dimensional slices through the system. This gives, however, a density which varies non-linearly in the distance to the edge of the domain. The reason for this untenable feature is as yet unresolved. It should also be noted that the limiting case of immobile B's has not been treated adequately in greater than one dimension. Indeed the self-similar spatial distribution of the B's has not yet been adequately analyzed.

3. Ballistic Single-Species Annihilation

3.1. Background

As alluded to in the introduction, there has been considerably less work on

ballistically-controlled reactions. Elskens and Frisch and independently Krug and Spohn [5] appear to be the first to determine the kinetics for the interesting situation of the ballistic "±" model in one dimension, where each particle velocity is $\pm v_0$ *i. e.*, the initial velocity distribution is $P(v, t = 0) = p\delta(v - v_0) + q\delta(v + v_0)$, with $q = 1 - p$. From rigorous probabilistic arguments, the density was found to decay as

$$c(t) \propto \sqrt{c(0)/vt}, \tag{17}$$

in the interesting case of $p = q = 1/2$. Elskens and Frisch also argued that this result can be understood qualitatively by consideration of density fluctuations in a linear domain of length ℓ. In such a region, there will typically be an imbalance in the number of right-moving and left-moving particles of magnitude $\delta n \simeq \sqrt{c(0)\ell}$. After a time $t = \ell/v$, only this residual fluctuation will remain inside the domain. Thus the concentration will be of order $c(t) \simeq \delta n/\ell$. By expressing ℓ in terms of t, Eq. (17) follows. This line of reasoning is closely analogous to the approach applied in diffusion-controlled two-species annihilation.

Our recent investigations[8] on ballistic annihilation represent logical extensions of the work of Elskens and Frisch to arbitrary initial velocity distributions. From analysis of the Boltzmann equation in the case of continuous velocity distributions, the density decays as $t^{-\alpha}$, with α dependent on the form of the initial velocity distribution and on the spatial dimension d. However, radically different behavior occurs for discrete initial velocity distributions. We also discuss the intriguing behavior that arises when there is superimposed diffusion on the primary ballistic motion.

3.2. Continuous velocity distributions

Consider a system of identical particles with a zero mean initial velocity distribution, $P(v, t = 0)$. (For simplicity, we consider a random initial spatial distribution.) Particles move at their initial velocity until a collision occurs, which results in the annihilation of both particles. We wish to determine the time dependence of the concentration, $c(t) = \int dv P(v, t) \sim t^{-\alpha}$, and the rms (or typical) velocity, $v_{\rm rms} = \left(\int dv\, v^2 P(v,t)/c(t)\right)^{1/2} \sim t^{-\beta}$.

From mean-free path considerations, the time between collisions for this system with particles of radius r and typical velocity $v_{\rm rms}$ at concentration c is $t \sim 1/cv_{\rm rms}r^{d-1}$, or $cv_{\rm rms} \propto t^{-1}$. Thus the relation $\alpha + \beta = 1$, which should hold for all spatial dimension d, follows. Since the lifetime of particles with velocity v is proportional to $1/v$, faster particles tend to annihilate more quickly, and the typical velocity should decay in time. Consequently α should typically be less than unity, and as shown below, its value depends on the form of the initial velocity distribution.

To determine the evolution of the velocity distribution in one dimension, we analyze the Boltzmann equation. Let $P(x, v, t)$ be the density of particles with velocity v at position x and at time t. At time $t + \Delta t$, the velocity distribution changes both because particles move and because of reactions. We treat the reaction

term in a mean-field approximation by first factorizing the 2-particle distribution as a product on single-particle distributions and assuming that a particle at $x' < x$ and velocity $v' > v$ necessarily reacts with the target particle at (x, v) when $x - x' < (v' - v)\Delta t$. There is a complementary contribution due to collisions between the target and a particle located at $x' > x$ with $v' < v$. These two contributions lead to[8]

$$P(x + v\Delta t, v, t + \Delta t) - P(x, v, t) =$$
$$- kP(x, v, t)\Big[\int_v^\infty dv' \int_{x-(v'-v)\Delta t}^{x} dx'\, P(x', v', t) + \int_{-\infty}^{v} dv' \int_{x}^{x+(v-v')\Delta t} dx'\, P(x', v', t)\Big], \tag{18}$$

where k is a dimensionless reaction constant. This approximate equation overcounts collisions, since the incident particle at x' may react with a third particle rather than with the target particle. We assume that the contributions of these three-body effects are negligible.

This Boltzmann equation can be simplified by expanding to first order in Δt and also assuming spatial homogeneity, so that the spatial derivative can be set to zero. This yields, for the concentration of particles with velocity v,

$$\frac{\partial P(v,t)}{\partial t} = -kP(v,t) \int_{-\infty}^{\infty} dv'\, |v - v'|\, P(v', t), \tag{19}$$

where the $|v - v'|$ dependence of the integral kernel controls the reaction rate. Although there are uncontrolled approximations underlying Eq. (19), this formulation gives a useful quantitative description of the decay kinetics.

This integral equation can be analyzed by scaling. We assume that the velocity distribution has the scaled form

$$P(v,t) = \frac{c_0}{v_0}\left(\frac{t}{t_0}\right)^{\beta-\alpha} f(z), \quad \text{with } z = \frac{v}{v_0}\left(\frac{t}{t_0}\right)^{\beta}, \tag{20}$$

where z is the dimensionless velocity, $t_0 = 1/(kc_0v_0)$ the initial time between reactions, k the dimensionless reaction constant, c_0 the initial concentration, and v_0 an initial typical velocity. Substituting this scaling form into Eq. (19), the exponent relation $\alpha + \beta = 1$ follows. Additionally, we obtain an equation for the scaling function

$$(2\beta - 1)f(z) + \beta z f'(z) = -f(z) \int_{-\infty}^{\infty} dz'\, |z - z'|\, f(z'). \tag{21}$$

By examining separately the large-z and small-z behavior of this equation, one can verify that an initial velocity distribution with a power-law tail at small velocities

leads to a scaling form for the time-dependent velocity distribution. Namely, if the initial velocity distribution has the form $P(v, t = 0) \propto |v|^\mu \theta(v_0 - |v|)$, where θ is the Heaviside step function, then it is possible to derive that $f(z)$ has the asymptotic forms $f(z) \sim z^\mu$ as $z \to 0$, and $f(z) \sim e^{-|z|/\beta}$ as $z \to \infty$. If we then make that ansatz that the full scaling function has the product form $|z|^\mu e^{-|z|/\beta}$, we then find $\beta = \frac{1}{3+2\mu}$.

Thus a scaling analysis of the Boltzmann equation predicts that α and β can take on any value between 0 and 1 as μ is varied, subject to the condition $\alpha + \beta = 1$. Notice that when the concentration decays relatively quickly, $\alpha \lesssim 1$, the typical velocity decays slowly, and *vice versa*. It is gratifying that the Boltzmann equation predictions turn out to be rather close to simulation results. This somewhat unexpected agreement stems from the relative absence of spatial and velocity correlations in the system. The generalization of the Boltzmann equation analysis to higher spatial dimensions yields $\beta = \frac{1}{1+2d+2\mu}$. Thus as the spatial dimension increases, the limiting value $\alpha = 1$, corresponding to the transparent limit, $\dot{c} = -kc^2$, is approached but never reached. Only in the $d = \infty$ limit are particle trajectories sufficiently independent that the typical velocity does not decrease. This is in contrast to many diffusion-controlled reactions for which transparent behavior occurs when $d \geq d_c$ with d_c finite.

3.3. Discrete velocity distributions

Unusual and incompletely understood features arise for discrete initial velocity distributions. In this case, the Boltzmann equation reduces to a finite set of (mean-field) rate equations. For many situations, these equations can be solved in closed form. While solutions to the Boltzmann equation and simulation results in one dimension are in good agreement for continuous velocity distributions, there are basic discrepancies in the corresponding results for discrete distributions. These discrepancies stem from the build up of long-range velocity correlations as the reaction proceeds. Thus it may be anticipated that the rate equations approach may not accurately describe the asymptotic behavior of one-dimensional systems with discrete initial velocity distributions.

To appreciate this situation in a generic case, consider, for example, the trimodal velocity distribution where $P(v, t = 0) = p_+\delta(v - 1) + p_0\delta(v) + p_-\delta(v + 1)$, with $p_+ + p_0 + p_- = 1$. For the symmetric case of $p_+ = p_-$, the Boltzmann equation for the concentrations of the stationary and mobile species, $c_0(t)$ and $c_\pm(t)$, respectively, reduces to the rate equations,

$$\dot{c}_0 = -2c_0c_\pm, \qquad \dot{c}_\pm = -c_0c_\pm - 2c_\pm^2. \tag{22}$$

The numerical factors of 2 are critical in the qualitative results. While the exact solution can be written in terms of the exponential integral, it is more instructive to write only the asymptotic behaviors,

$$c_\pm(t) \sim \frac{1}{2}c_0(\infty)\, e^{-c_0(\infty)t}, \qquad c_0(t) \sim c_0(\infty) \exp\left[e^{-c_0(\infty)t}\right]. \tag{23}$$

where, $c_0(\infty) = c_0(t=0)\, e^{-2c_\pm(0)/c_0(0)}$. According to the rate equations, the concentration of mobile particles decays exponentially in time, while a residue of stationary particles always remains whose concentration is vanishingly small if the initial concentration is relatively small.

Numerical simulations of this process in one dimension indicate a rather different behavior. Because of subtle crossover effects, a direct simulation turns out to be inadequate to yield accurate results. We therefore developed an approach in which all collision partners and the corresponding collision times are identified at the outset. With this method we can simulate 5×10^5 particles to 10^5 time steps in of the order of 30 cpu seconds on a DEC/AXP 3000/400 workstation. These simulations reveal the following: For $c_0(0) < 1/4$, $c_0(t) \sim 1/t$ and $c_\pm(t) \sim t^{-1/2}$, but with the asymptotic behavior setting in more slowly as $c_0(0)$ is increased. When $c_0(0) = 1/4$, $c_0(t) = c_\pm(t) \sim t^{-2/3}$. For $c_0(0) > 1/4$, $c_0(t)$ saturates to a finite limiting value which appears to be proportional to $(c_0(0) - \frac{1}{4})^2$, while $c_\pm(t)$ decays faster than a power law.

The two different exponent values for the case $c_0(0) < 1/4$ can be understood in the limit of $c_0(0) \to 0$. For an infinitesimal concentration of stationary "impurities", the moving particles react among themselves with overwhelming probability and the system reduces to the $\pm$ model for which $c_\pm(t) \sim t^{-1/2}$. On the other hand, a stationary particle survives only if it is not annihilated by particles incident from either direction. Since the probabilities of each of these two events is independent, it follows that $c_0(t) \sim c_\pm(t)^2 \sim t^{-1}$ in the limit $c_0(0) \ll c_\pm(0)$.

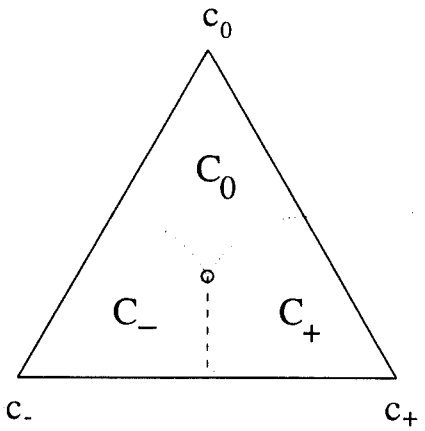

Figure 3. "Phase" diagram of the one-dimensional 3-velocity model in the triangle defined by the relative concentrations of the three species. Along the dashed line, $c_\pm(t) \sim t^{-1/2}$, while $c_0(t) \sim t^{-1}$. At the point marked by the small circle, $c_\pm(0)=3/8$, $c_0(0)=1/4$, all species decay as $t^{-2/3}$. Along the dotted lines, the nature of the decay is unknown, except very close to the extrema which correspond to the "fast impurity" problem (see below). The letters in the interior of the triangle indicate the dominant species in the long-time limit.

This interesting limiting result motivates consideration of the general situation where the initial concentrations of the three species is arbitrary. In this case, we can

account for some aspects of the "phase" boundaries in the two-dimensional phase plane spanned by the relative concentrations of the three species (Fig. 3). Here, the term "phase" refers to the situation where a single species dominates in the long time limit. The results of the previous paragraph pertain to the boundary between the + phase (dominated by right-moving particles) and a − phase, where the decay of the concentration of 0's (stationary particles) is the most rapid. The complementary situation of the decay of −'s along the boundary between the + and 0 phase also exhibits peculiar characteristics. For simplicity, consider an infinitesimal concentration −'s in a background of equal concentrations of 0's and +'s. By a Galilean transformation, this is equivalent to a "fast impurity" problem, that is, the survival probability of a single fast impurity which moves in a symmetric ± background. A heuristic argument suggests that this survival probability decays slower than an exponential but faster than a power law in time.

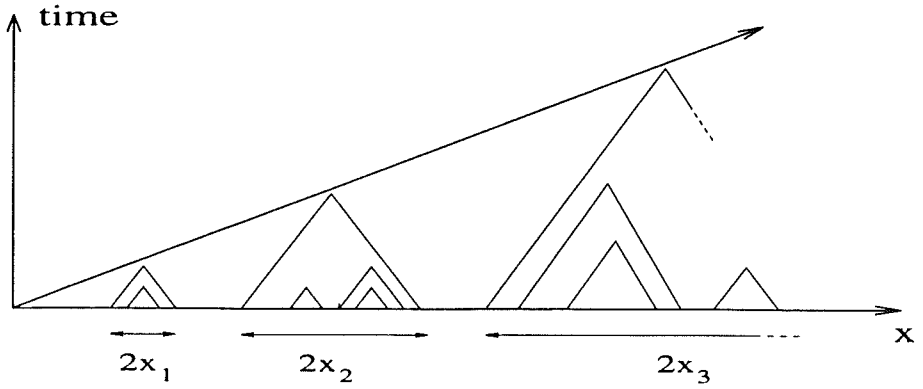

Figure 4. World line of a fast impurity in a background of equal concentrations of background ± particles. Successive triangles of self-annihilating background particles are indicated.

The basis of this argument is to consider the subset of configurations which give the dominant contribution to the survival probability of the fast impurity, but which are sufficiently simple to permit an asymptotic evaluation of this probability. In order for the impurity to survive to time t, the background ± particles must annihilate among themselves up to this time. On a space-time diagram these self-annihilation events appear as a sequence of isosceles triangles which do not extend to the world line of the impurity. We claim that the dominant contribution to the survival probability stems from the systematic sequence of ever-larger self-annihilation triangles which just miss the impurity world line. From basic geometry, the base of the n^{th} triangle $x_n \propto ((v_0+1)/(v_0-1))^n \equiv \beta^n$. Additionally, the number of triangles that comprise the self-annihilation sequence up to time t is just $N \simeq \ln t/\ln\beta$. Finally, a self-annihilation triangle of base x_n occurs with probability $x_n^{-3/2}$. This latter result merely reflects the fact that the probability of a particle annihilating with its n^{th} neighbor decreases as $n^{-3/2}$ for large n. The impurity survival probability $S(t)$ is simply the product of the occurrence probabilities of the sequence of

self-annihilation triangles. Putting the above factors together, we find,

$$S(t) \sim \prod^{\ln t/\ln\beta} (2x_0\beta^n)^{-3/2} \propto \beta^{-3n^2/4} \sim \exp(-\ln^2 t/\tfrac{4}{3}\ln\beta). \tag{24}$$

As a byproduct of this result, it is straightforward to show that the mean lifetime of the impurity is proportional to $(\frac{v_0+1}{v_0-1})^{2/3}$. Both of these unusual results are in excellent agreement with numerical simulations.

3.4. Mixed ballistic and diffusive motion

For a discrete initial velocity distribution, particles with the same velocity never meet. However, superimposed diffusion permits same-velocity particles to annihilate, a mechanism which leads to interesting behavior. Thus consider again the $\pm$ model, in which each particle undergoes superimposed diffusion, with diffusion coefficient D, in addition to the $\pm v_0$ ballistic motion. The resulting kinetics can be treated by dimensional analysis. Using the parameters of the system, the initial concentration c_0, the velocity v_0, and the diffusion coefficient D, the only variable combinations with the dimensions of concentration are, c_0, $1/v_0t$, and $1/\sqrt{Dt}$. Accordingly, the time dependent concentration can be anticipated to have the form

$$c(t) \propto (c_0)^\mu \left(\frac{1}{v_0 t}\right)^\nu \left(\frac{1}{\sqrt{Dt}}\right)^{1-\mu-\nu}. \tag{25}$$

We determine μ and ν by requiring that $c(t)$ matches with the known limiting behaviors in the cases of negligible drift[12] and negligible diffusion[5] at the appropriate crossover times. In the former case Eq. (25) should reduce to the diffusion-limited result $c(t) \to (Dt)^{-1/2}$ when $t < \tau_v \simeq D/v_0^2$, the crossover time below which drift effects can be ignored. Conversely, in the limit of small D, Eq. (25) should reduce to $c(t) \to (c_0/v_0t)^{1/2}$ for $t < \tau_d \simeq 1/(Dc_0^2)$, which is the time for adjacent particles to meet by diffusion. By straightforwardly matching the general result Eq. (25) to the aforementioned limiting behaviors at the appropriate crossover times, we find

$$c(t) \sim \left(\frac{1}{v_0 t}\right)^{1/2} \left(\frac{1}{\sqrt{Dt}}\right)^{1/2} \propto t^{-3/4}. \tag{26}$$

Interestingly, the density decays as $t^{-1/2}$ for both the diffusion-limited and the ballistically-limited reactions, but the combination of both mechanisms leads to a faster $t^{-3/4}$ decay of the density.

4. Summary

In diffusion-limited two-species annihilation, an initially homogeneous distribution of A's and B's at equal initial densities evolves into a mosaic of growing single

species domains. When both species are equally mobile, the concentration within the domain core is roughly uniform and proportional to $t^{-d/4}$, while the concentration vanishes linearly in the distance to the domain edge for spatial dimension $d \leq 2$. This linear decay leads to a new length scale, ℓ_{AB}, intermediate to the typical interparticle spacing and the typical domain size, as well as multiscaling in the reduced moments $\langle \ell_{AA}^n(t) \rangle^{1/n}$. When one species is immobile, the domains of immobile species evolve only by infiltration of mobile species from the exterior, and vestiges of the initial distribution persist in the domain interior. This leads to a power law distribution for the separations of the immobile particles in which, $\langle \ell_{BB}^n(t) \rangle^{1/n}$ appears to increase as a power law in time for $n \geq 1/2$, but approaches a finite limiting value for $n < 1/2$.

In higher dimensions, there is less understanding of the domain structure and of the spatial organization of reactants. Numerical evidence indicates that anomalous scaling of interparticle distances exists in $d = 2$ but not in $d = 3$. Thus $d = 3$ appears to be a critical dimension above which there is no substantial depletion layer at the periphery of a domain.

Ballistically-controlled single-species annihilation, $A+A \to 0$ exhibits a rich phenomenology which depends on the form of the initial velocity distribution. Analysis of the Boltzmann equation for continuous initial velocity distributions indicates that the time dependence of the concentration and the typical velocity are governed by exponents whose values depend on the small-velocity limit of the initial velocity distribution. Intriguingly, an initial velocity distribution with a large component of slower particles gives a weak decay of the concentration and relatively faster decay of the typical velocity. As the spatial dimension is increased, the "transparent" limit $a = 1$ is approached but apparently never reached.

For discrete velocity distributions, there is intriguing long-time behavior. In the 3-velocity model, a combination of asymptotic arguments and numerical simulations indicates that different species decay at different power law rates for appropriate initial conditions. The full range of phenomenology is ripe for further exploration. In the case of combined ballistic and diffusive reactant motion, the concentration decays more rapidly than in the cases where only one transport mechanism is operative. This interesting behavior can be accounted for by dimensional analysis. However, a microscopic theory has yet to be developed.

5. Acknowledgements

I wish to thank E. Ben-Naim, P. Krapivsky, and F. Leyvraz for pleasant collaborations that led to the work reported here, and D. Dhar for helpful discussions. I also gratefully acknowledge ARO grant DAAH04-93-G-0021, NSF grants INT-8815438 and DMR-9219845, and the Donors of The Petroleum Research Fund, administered by the American Chemical Society, for partial support of this research.

6. References

1. For recent reviews on two species annihilation see *e. g.*, Ya. B. Zeldovich, A. S. Mikhailov: *Sov. Phys. - Usp.* **30** (1988) 23; R. Kopelman: *Science* **241** (1988) 1620; A. A. Ovchinnikov, S. F. Timashev, A. A. Belyy: *Kinetics of Diffusion Controlled Chemical Processes* (Nova Science Publishers, 1990); S. Redner and F. Leyvraz, in *Fractals and Disordered Systems,* Vol. 2, S. Havlin, A. Bunde, Editors (Springer, Heidelberg, 1994).
2. Ya. B. Zeldovich, A. A. Ovchinnikov: *Chem. Phys.* **28** (1978) 215; S. F. Burlatskii, A. A. Ovchinnikov: *Russ. J. Phys. Chem.* **52**, 1635 (1978).
3. See *e. g.*, D. Toussaint and F. Wilczek, *J. Chem. Phys.* **78** (1983) 2642.
4. K. Kang, S. Redner: *Phys. Rev. Lett.* **52** (1984) 955; *Phys. Rev. A* **32** (1985) 435.
5. Y. Elskens and H. L. Frisch, *Phys. Rev. A* **31** (1985) 3812; J. Krug and H. Spohn, *Phys. Rev. A* **38** (1988) 4271.
6. G. F. Carnevale, Y. Pomeau and W. R. Young, *Phys. Rev. Lett.* **64** (1990) 2913.
7. Y. Jiang and F. Leyvraz, *J. Phys. A* **26** (1993) L179.
8. E. Ben-Naim, S. Redner, and F. Leyvraz, *Phys. Rev. Lett.* **70** (1993) 1890.
9. F. Leyvraz, S. Redner, *Phys. Rev. Lett.* **66** (1991) 2168; *Phys. Rev. A* **46** (1992) 3132.
10. See *e. g.*, L. D. Landau, E. M. Lifshitz: *Quantum Mechanics* (Pergamon Press, New York, 1977).
11. F. Leyvraz: unpublished notes; D. ben-Avraham: *J. Chem. Phys.* **88** (1988) 941; M. E. Fisher, M. P. Gelfand: *J. Stat. Phys.* **53** (1988) 175.
12. D. C. Torney, H. M. McConnell: *Proc. Roy. Soc. London Ser. A* **387**, (1983) 147; A. A. Lushnikov: *Sov. Phys. JETP* **64**, (1986) 811.